

# Characterization of the Gas Tungsten Arc Welded $\text{Cu}_{54}\text{Ni}_6\text{Zr}_{22}\text{Ti}_{18}$ Bulk Metallic Glass Weld

Jonghyun Kim<sup>1,\*</sup>, Seungyong Shin<sup>1</sup> and Changhee Lee<sup>2</sup>

<sup>1</sup>R&D Division for Bulk Amorphous and Nano Materials, Korea Institute of Industrial Technology, 994-32, Dongchun-Dong, Yeonsu-Gu, Incheon 406-130, Korea

<sup>2</sup>Division of Materials Science & Engineering, Hanyang University, 17 Haengdang-dong, Seongdong-ku, Seoul 133-791, Korea

Gas tungsten arc welding is well-established joining process for the structural materials. Due to the localized heat input, the non-uniform temperature distribution in weld is inevitable. In this regard, the thermal instability of the bulk metallic glass [BMG] should be considered for the weldability. Microstructure and phase evolutions of the  $\text{Cu}_{54}\text{Ni}_6\text{Zr}_{22}\text{Ti}_{18}$  BMG weld were investigated and the fusion welded BMG weld is defined and the solid-state crystallization of the heat affected zone made the weld brittle. Furthermore, the thermal stress induced crack was propagated along the crystallized heat affected zone.

(Received March 14, 2005; Accepted May 16, 2005; Published June 15, 2005)

**Keywords:**  $\text{Cu}_{54}\text{Ni}_6\text{Zr}_{22}\text{Ti}_{18}$  bulk metallic glass, Gas tungsten arc welding, Heat affected zone

## 1. Introduction

There have been many studies for developing higher glass formable bulk metallic glass [BMG], evaluating material properties, and designing hybrid BMG materials and it has been proved that BMG shows high specific strength/hardness and superior localized corrosion resistance.<sup>1-3)</sup> However, monolithic BMG materials are brittle and the uncontrolled crystallization further increases the brittle nature. In order to enlarge the applicability of the BMG for the structural applications, the joining process should be developed. Among various kinds of joining processes, the fusion welding is a well-established joining process and can be classified to gas welding, arc welding and high energy density welding according to the heat source. Gas tungsten arc welding is a well-known autogeneous fusion welding process of the arc welding processes. Arc, which is generated between a thoriated tungsten electrode and a substrate, is used to heat and melt the substrate. When it comes to the high energy density welding, such as the electron beam welding and the laser welding, the absolute heat input is much lower than both the gas welding and the arc welding but the input energy is focused to a highly localized area about millimeter scale. As a matter of fact, it was suggested that the weldability of the bulk metallic glass by the high energy density welding process such as electron beam welding is applicable for joining the bulk metallic glass without the crystallization during welding.<sup>4,5)</sup> However, the process is very expensive and it is not so simple as gas welding and arc welding. As far as the weldability of gas tungsten arc welded BMG may be concerned, thermal history and phase evolution are very important. Due to the localized heat input, the fusion weld is generally composed of weld metal, heat affected zone, and base metal.

In this study,  $\text{Cu}_{54}\text{Ni}_6\text{Zr}_{22}\text{Ti}_{18}$  BMG [the glass forming ability of 6 mm] plate was produced by roll-casting method and the plate was welded by the micro-gas tungsten arc welding [bead-on-plate]. Gas tungsten arc welded BMG weld

Table 1 Characteristics of the as-rolled  $\text{Cu}_{54}\text{Ni}_6\text{Zr}_{22}\text{Ti}_{18}$  BMG plate.

$\text{Cu}_{54}\text{Ni}_6\text{Zr}_{22}\text{Ti}_{18}$	T <sub>g</sub> (K)	T <sub>x</sub> (K)	ΔT <sub>x</sub> (K)	T <sub>rg</sub> (T <sub>g</sub> /T <sub>m</sub> <sup>liq</sup> )
Ribbon	712	769	57	0.55
Plate	713	769	56	0.55

was intensively investigated and the BMG weld is defined in view of the phase composition.

## 2. Experiment

$\text{Cu}_{54}\text{Ni}_6\text{Zr}_{22}\text{Ti}_{18}$  BMG plate was manufactured using an arc melting and rolling process.<sup>6)</sup> Arc melted base alloy was re-melted by electrical arc and then the melt was subsequently rolled before solidifying within an argon gas environment. Specimens with 1.0 mm thickness, 100 mm in width and length were prepared. The phase composition was identified by the X-ray diffractometry and the thermal properter of the as-rolled BMG plate were observed using the differential scanning calorimetry at a heating rate of 0.67 Ks<sup>-1</sup>. Characteristics of the as-rolled BMG plate were compared with those of a melt-spun ribbon (Table 1). Before welding, BMG plate was ultrasonically cleaned and dried using Ar gas. Heat input was 0.44, 0.88, 1.32 and 1.76 J/m: arc voltage of 11 V, arc currents of 5, 10, 15 and 20 A, and travel rate of 12.5 mm/s. After welding, the cross-sectional morphology of the weld was observed using a scanning electron microscope equipped with an energy dispersive spectroscope. Also, the phase composition of the cross-section of the welded BMG was investigated using a micro-area X-ray diffractometer. The diameter of the collimator was 50 μm. In order to qualitatively estimate the mechanical properties of the BMG weld, nano-indentation was conducted on the cross-section at the maximum load of 0.049 N.

## 3. Results and Discussion

Figure 1 shows the effects of the heat input on the weld morphology and the crystallization behaviors of both the weld metal and the heat affected zone in the gas tungsten arc

\*Graduate Student, Hanyang University

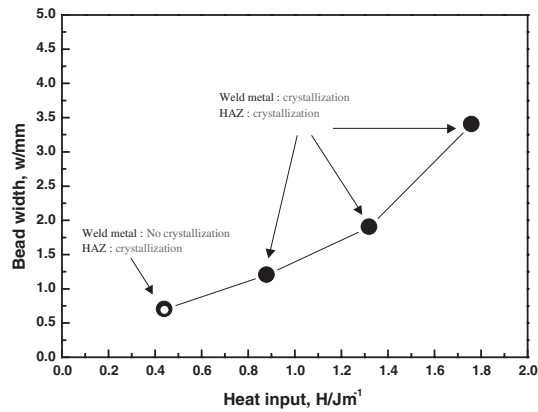


Fig. 1 Bead widths of gas tungsten arc welded  $\text{Cu}_{54}\text{Ni}_6\text{Zr}_{22}\text{Ti}_{18}$  BMG according to heat input.

welding of the  $\text{Cu}_{54}\text{Ni}_6\text{Zr}_{22}\text{Ti}_{18}$  BMG. Weld width is increased with the increase of the heat input and the full penetration can be obtained at no less than 1.44 J/m. Regardless of the heat input, the crystallization is inevitable in the heat affected zone. Meanwhile, the crystalline phase was absent in the weld metal which was produced by the heat input of 0.44 J/m.

Macro cross-sectional morphology and phase distribution of the gas tungsten arc welded  $\text{Cu}_{54}\text{Ni}_6\text{Zr}_{22}\text{Ti}_{18}$  BMG at the heat input of 0.44 J/m are seen in Fig. 2. BMG weld can be divided into three regions as marked A, B and C. Marked A region is the weld metal where the peak temperature is above

the melting point. From the microstructure and the diffraction pattern, the cooling rate of the weld metal is faster than the critical cooling rate for suppressing the crystallization during cooling of the liquid BMG: a critical cooling rate of the  $\text{Cu}_{54}\text{Ni}_6\text{Zr}_{22}\text{Ti}_{18}$  can be estimated by other  $\text{CuNiZrTi}$  quaternary BMG alloys<sup>7)</sup> and it is about  $27.7 \text{ K s}^{-1}$  considering the critical thickness of 6 mm. However, particulate phases are shown in the marked B region showing dark contrast and sharp crystalline peaks are present in the X-ray diffraction pattern. This region can be regarded as the heat affected zone from the viewpoint of the conventional welding metallurgy. During welding, the peak temperature was below the solidus line of the BMG due to the localized heat input and heat conduction. The solid-state crystallization of the undercooled liquid BMG is affected by the thermal cycle. In this case, the accumulated duration time in the high temperature is longer than the incubation time for the crystallization during reheating and cooling. Marked C region is considered to be the base metal where the peak temperature seems to have been below the crystallization temperature. For the effects of the heat input on the characteristics of the BMG weld, dimensions of the weld metal and the crystallized heat affected zone were increased with the heat input. Also micro and macro cracking are observed within the crystallized heat affected zone because of the thermal stress arising from the localized heat input as shown in Fig. 3. As a matter of fact, the spontaneous fracture resulted from the thermal stress within the crystallized heat affected zone at the heat input of 1.76 J/m.

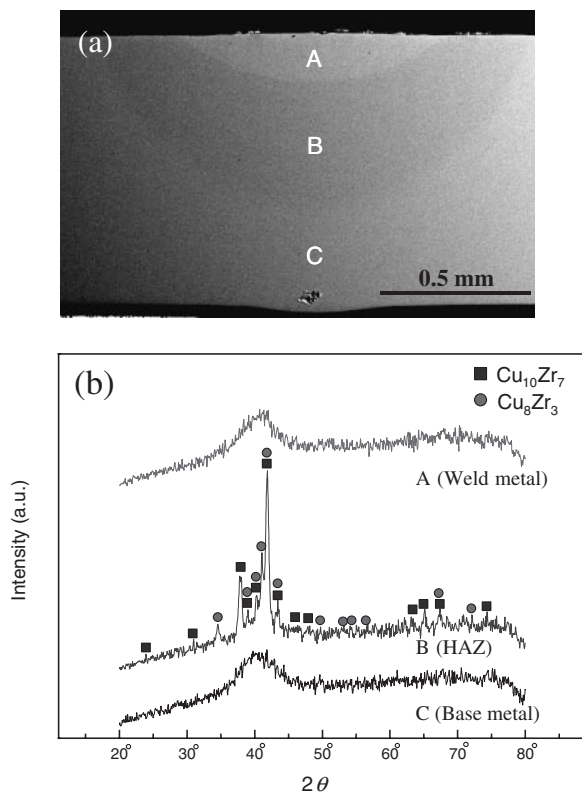


Fig. 2 Characteristic features of the gas tungsten arc welded BMG at the heat input of 0.44 J/m. (a) Overall cross-sectional morphology of the as-welded  $\text{Cu}_{54}\text{Ni}_6\text{Zr}_{22}\text{Ti}_{18}$  BMG weld. (b) X-ray diffraction in marked A, B and C region.

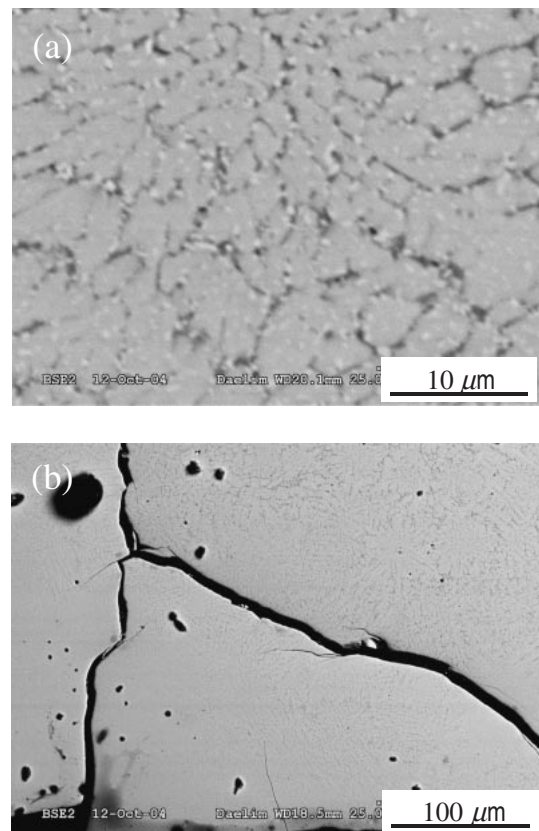


Fig. 3 Micro and macro cracking of the as welded BMG. (a) Micro-cracking (0.88 J/m). (b) Macro-cracking (1.32 J/m).

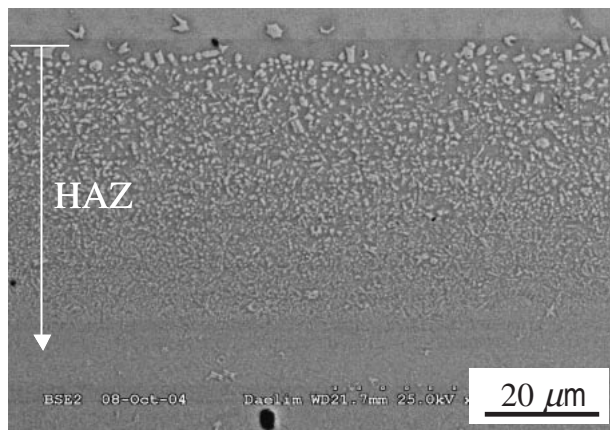


Fig. 4 Closer look of the heat affected zone of the  $\text{Cu}_{54}\text{Ni}_6\text{Zr}_{22}\text{Ti}_{18}$  BMG weld at the heat input of 0.44 J/m.

In Fig. 4, the crystallization behavior in the heat affected zone can be seen. Though the glassy phase is thermodynamically unstable, the randomly packed atomic configuration is retained due to the negligible rate of the atomic diffusion below the glass transition temperature. However, atoms spontaneously move to achieve long range order for the stable crystalline when the sufficient energy is provided by either the thermal energy<sup>8)</sup> or the mechanical energy.<sup>9)</sup> During welding, the energy overcoming the activation barrier for the crystallization is given by the thermal energy and the crystallization behavior is considered to follow the solidification of the crystalline phase from the liquid. With the presence of the temperature gradient, the nucleation rate and the growth rate are dependent on the temperature. As the temperature is decreased (the distance from the fusion boundary is increased), the undercooling degree is increased while the atomic diffusivity is decreased. In this regard, as the distance from the fusion line is increased, the crystalline phase number density is increased but the size is decreased: network of random microcracks among crystalline phases are seen in Fig. 3(a) and macro-cracks penetrate the crystallized heat affected zone. Through the microstructural features, it can be deduced that the crystallization of the BMG during welding makes heat affected zone brittle as can be expected from the other literature sources dealing with the detrimental effects of the crystallization on the mechanical properties.

Though the effects of the crystallization of the BMG on the

mechanical properties are dependent on the crystallinity and the crystalline phase size, the crystallization generally deteriorates the mechanical properties due to the embrittlement. For the BMG weld, the hardness variation is actually affected by the crystallization. The hardness value is sharply increased near the interface between the weld metal and the heat affected zone and then decreased. Nano-hardness of the weld metal was Hv 550 which is similar to that of the base metal while that of the heat affected zone was about Hv 650.

#### 4. Conclusions

Through this study, it can be suggested that the BMG weld by the gas tungsten arc welding is composed of the weld metal, the crystallized heat affected zone, and the base metal. Crystallization of the BMG weld can be divided into two parts due to the localized heat input: the weld metal and the heat affected zone. For the weld metal in which the crystallization is determined by the effective cooling rate of the molten liquid, it could be assumed that the cooling rate of the molten liquid was decreased to be higher than the critical cooling rate as the heat input was increased. On the other hand, the solid-state crystallization during reheating thermal cycle was unavoidable within the scope of this study.

#### Acknowledgement

This work was supported by the Next Generation—New Technology Development Program of the Ministry of Commerce, Industry and Energy in Korea.

#### REFERENCES

- 1) A. Inoue: *Acta Mater.* **48** (2000) 279–306.
- 2) A. Inoue, N. Nishiyama and T. Matsuda: *Mater. Trans.* **37** (1996) 181–184.
- 3) A. Peker and W. L. Johnson: *Appl. Phys. Lett.* **63** (1993) 2342–2344.
- 4) Y. Kawamura and Y. Ohno: *Mater. Trans.* **42** (2001) 2476–2478.
- 5) Y. Kawamura, S. Kagao and Y. Ohno: *Mater. Trans.* **42** (2001) 2649–2651.
- 6) S. Y. Shin, J. H. Kim, D. M. Lee, J. K. Lee, H. J. Kim, H. G. Jeong and J. C. Bae: *Mater. Sci. Forum.* **449–452** (2004) 945–948.
- 7) C. C. Hays and S. C. Glade: *Appl. Phys.* **80** (2002) 3096–3098.
- 8) K. Samwer, R. Busch and W. L. Johnson: *Phys. Rev. Lett.* **82** (1999) 580–583.
- 9) J. Zhang, Y. H. Wei, K. Q. Qiu, H. F. Zhang, M. X. Quan and Z. Q. Hu: *Mater. Sci. Eng. A.* **375** (2003) 386–391.